Robot Sonar Mapping by Bayesian Search

Kenneth D. Harris
Department of Anatomy and Developmental Biology
University College London
Gower Street, London WC1E 6BT, UK
kdh@anat.ucl.ac.uk

Michael Recce
Department of Computer Science
New Jersey Institute of Technology
University Heights, Newark NJ, USA
michael@ncrl.njit.edu

Abstract

This paper describes a new method by which a mobile robot can construct a map of its environment from sonar sensory data. A model of sensor behaviour is used to construct a probability function on the space of all maps, which is then searched for the map of highest probability. Because of the very large dimension of this space, specialised search techniques are required. The algorithm was tested on real sonar data collected in three heterogeneous environments, and the quality of maps produced by the new method were quantitatively compared to those of two previous mapping systems.

Introduction

Sonar sensors have proved popular in mobile robotics due to their low cost and flexibility of use. The output of sonar rangefinders is, under the right circumstances, an accurate and reliable measurement of distance to obstacles. However, the behaviour of these sensors is not always straightforward, and this has lead to difficulty in sonar mapping, particularly in the presence of specular walls.

Previous sonar mapping systems have fallen into two classes. The first class of *feature-based* mapping systems (Leonard & Durrant-Whyte 1992; Lee & Recce 1997) represent the map of space by a collection of features, which correspond to physical objects in the environment. The positions of these features are determined using heuristics, rather than mathematical principles. These algorithms therefore contain many free parameters, and may not be optimal in any sense.

In the second class of *grid-based* mapping systems (Elfes 1987; Moravec 1988), the robots environment is overlaid with a square grid, and a number is stored for every grid segment representing the occupancy probability for that segment. The rules for updating of occupancy probabilities are derived from Bayes' theorem. However, an incorrect assumption of independence of occupancy of grid segments is made.

This independence assumption must be made, because grid-based mapping methods are *incremental* methods, meaning that an *a posteriori* probability distribution is stored in memory, and updated as new sonar data arrives. By making the independence assumption, the probability distribution can be represented by a single probability for each segment. Without the independence assumption, a probability would need to be stored for every single possible map configuration. This is clearly impractical as the number of possible configurations is exponential in the number of grid segments.

Recent work has sought to extend grid-based mapping within an incremental framework (Lim & Cho 1992; Harris & Recce 1997; Konolige 1997; Thrun 1998). In this paper we adopt a non-incremental approach, in which a record of all sensory readings is kept, and these are used to construct a probability function on the space of all maps, which is then searched for the map of maximum *a posteriori* probability. The space of all maps is very large, but with a suitable choice of feature-based map representation, it has a structure that makes an approximate global search computationally tractable.

General Formalism

The mapping system described in this paper is a prescription for generating a map given a history of measurements. Each measurement α is characterised by transducer location $\xi_\alpha = (x_\alpha, y_\alpha, \theta_\alpha)$, and measured range R_α. We consider the transducer locations $\{\xi_\alpha\}$ to be fixed, but the ranges $\mathcal{R} = \{R_\alpha\}$ to be random variables. We assume that the output of the rangefinder is discrete. We model the robot's environment as consisting of a set of features $\mathcal{F} = \{F_i : i = 1 \ldots N_f\}$, each of which is characterised by a feature type and location.

By Bayes' theorem, the probability of a map $\{f_i\}$ given a set of readings $\{r_\alpha\}$ is given by

$$P(\mathcal{F} = \{f_i\} | \mathcal{R} = \{r_\alpha\}) = \frac{P(\mathcal{R} = \{r_\alpha\} | \mathcal{F} = \{f_i\}) P(\mathcal{F} = \{f_i\})}{P(\mathcal{R} = \{r_\alpha\})} \quad (1)$$

To produce a map for a given measurement history, we must find the feature configuration $\{f_i\}$ that maximises this expression. Since the denominator does not depend on $\{f_i\}$, we may ignore it. $P(\mathcal{F} = \{f_i\})$ is a prior distribution, which we model by a prior $P_f(f)$ on

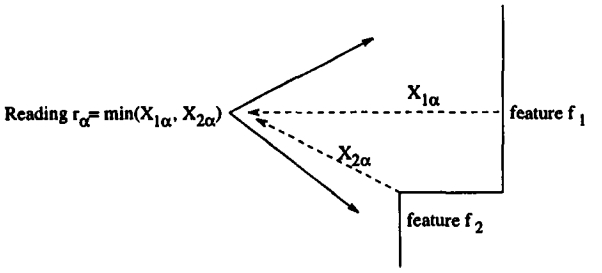

Figure 1: The model for how environmental features interact to produce a sonar reading. Each feature f_i produces an echo $X_{i\alpha}$ in response to sonar beam α. The range measured by the sensor is $min_i(X_{i\alpha})$, the smallest of the echos. In the situation shown in the figure, the echo from the corner f_2 is shorter than the echo from the wall f_1, so the sensor measures the distance to the corner, $X_{2\alpha}$.

the position of each feature, and a Poisson distribution on the number of features (with mean $\lambda = 10$):

$$P(\mathcal{F} = \{f_i\}) = \frac{e^{-\lambda}\lambda^{N_f}}{N_f!}\prod_{i=1}^{N_f} P_f(f_i) \qquad (2)$$

We want our choice of $P_f(f_i)$ to have minimal effect on the results of the mapping system. In Bayesian theory, such a prior is called a *reference prior* (Antelman 1997), and will be approximated by a flat distribution. A flat distribution over a continuous variable is *improper*, i.e. cannot be normalised to have total probability 1, but may be taken as a limiting case.

In order to model $P(\mathcal{R} = \{r_\alpha\}|\mathcal{F} = \{f_i\})$, we need a model of the way environmental features interact to produce range readings. Our model is illustrated in figure 1. For each range reading α, a feature F_i may produce an echo, which arrives back at the transducer with time delay corresponding to a distance of $X_{i\alpha}(F_i, \xi_\alpha)$ (If the feature does not produce a reflection, $X_{i\alpha}$ is defined to be infinity). The range reported by the sensor corresponds to the first echo to arrive at the sensor, and therefore will be $min_i(X_{i\alpha})$. In order to account for sensory noise, the $X_{i\alpha}$ are modelled by stochastic functions of feature position. We assume that the $X_{i\alpha}$ are independent for a given feature configuration $\{F_i\}$. The set of R_α are therefore also independent for a given feature configuration.

Now, because $R_\alpha = min_i(X_{i\alpha})$, R_α will take the value r when all the $X_{i\alpha}$ are greater than or equal to r, but they are not all strictly greater than r. By independence of the $X_{i\alpha}$:

$$P(R_\alpha = r) = \prod_i P(X_{i\alpha} \geq r) - \prod_i P(X_{i\alpha} > r) \qquad (3)$$

We define the *map score* of a map $\{f_i\}$ given a set of readings $\{r_\alpha\}$ to be the log of the *a posteriori* probability of a feature configuration. Using equations 1, 2, and 3, the independence of the $\{R_\alpha\}$, and the flat approximation to $P_f(f)$, this may be written as:

$$\begin{aligned} SC_{map}(\{f_i\};\{r_\alpha\}) &= logP(\mathcal{F} = \{f_i\}|\mathcal{R} = \{r_\alpha\}) \\ &= const + \textstyle\sum_\alpha SC_{reading}(r_\alpha;\{f_i\}) + logP(N_f) \end{aligned} \qquad (4)$$

Where $SC_{reading}(r_\alpha;\{f_i\})$ is the *reading score* of a reading r_α, given a map $\{f_i\}$:

$$SC_{reading}(r_\alpha;\{f_i\}) = log\left[\prod_i P(X_{i\alpha} \geq r_\alpha) - \prod_i P(X_{i\alpha} > r_\alpha)\right] \qquad (5)$$

Physical Model

In order to evaluate $SC_{reading}(r_\alpha;\{f_i\})$, we need to know the probability distribution of $X_{i\alpha}(f_i, \xi_\alpha)$ for a given feature f_i and sensor position ξ_α. We have previously created a model for this probability distribution from experimental sonar data (Harris & Recce 1998; Harris 1998; 1999)

In this model, there are three types of feature: specular and rough walls, and point-like sharp edges. In all cases, the modelled sensor output comes from the same family of probability distributions. A distribution in this family is specified by three parameters, p, μ, and σ, where p is the probability that the sensor will detect a reflection from the feature in question, and μ and σ giving the mean and standard deviation of a normal distribution for returns in the case that a return is received. The equations for the values of these parameters are given in the appendix.

The modelled probability distributions are continuous, but the actual readings made by the sonar sensor are discrete, with 1cm bin resolution. We calculate the probability that $X_{i\alpha}$ will lie in a given range bin by the integral of the probability density over that bin. Because the modelled distribution is Gaussian, this integral may be computed analytically.

Effect of wall endpoints

The probability distributions in the appendix model returns from a wall as a function of perpendicular distance and beam incidence angle but not lateral displacement along the wall.

The model we will use for the effect of wall endpoints takes into account the finite width of the sonar beam, and is illustrated in figure 2. We consider a beam of half-width 0.25 radians, centred on the returning sonar radiation at angle θ_r. For rough walls, θ_r is given by equation 7, and for specular walls θ_r is zero. If any part of this beam intersects the wall, then a reflection is produced with probability p given by the models of the appendix; if not, no reflection is produced, and $p = 0$.

Mean-field approximation

We have recast the problem of map construction as global optimisation of $SC_{map}(\{f_i\};\{r_\alpha\})$ over the space

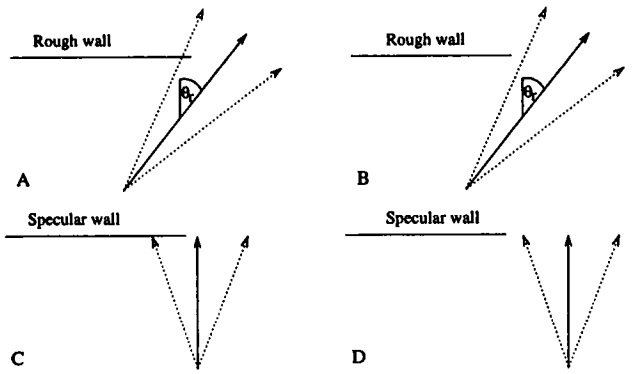

Figure 2: The model for the effect of wall endpoint positions. For rough walls, a reflection is produced if any part of the wall intersects any part of a sonar beam of half-width 0.25 radians centred on the returning radiation direction θ_r; so a reflection will be produced in (A) but not (B). For specular walls, a reflection is produced if any part of the wall intersects any part of a sonar beam of half-width 0.25 radians centred on the perpendicular line from the sensor position to the wall; so a reflection is produced in (C) but not (D).

of all maps $\{f_i\}$. There could be of the order of 50 features, leading to a optimisation problem of up to 200 continuous dimensions. Unfortunately, global optimisations of this size are very difficult problems, with no general solution.

To make the search tractable, we will use a "mean-field" approximation to find the positions of plausible features in the environment, and then choose a subset of these features that gives a high map score. We will define the *mean field* score of a feature f_0 to be the log likelihood of the observed readings given the presence of the *single* feature f_0 in the map $\mathcal{F}$:

$$SC_{mf}(f_0; \{r_\alpha\}) = logP(\mathcal{R} = \{r_\alpha\} | f_0 \in \mathcal{F})$$

Every f_0 that locally maximises this function will correspond to a plausible single feature.

It is possible to explicitly compute this score by performing a sum over all maps that contain the feature f_0 (Harris 1999). The result is:

$$SC_{mf}(f_0; \{r_\alpha\}) = \sum_\alpha log\left[A_\alpha P(X_{0\alpha} \geq r_\alpha) - B_\alpha P(X_{0\alpha} > r_\alpha)\right] \quad (6)$$

The numbers A_α and B_α depend only on the observed range r_α, and can be interpreted as the probability that an "average" feature causes a reading greater than or equal to r_α, or greater than r_α, respectively. The calculation of these numbers is given by a simple formula, derived in (Harris 1999).

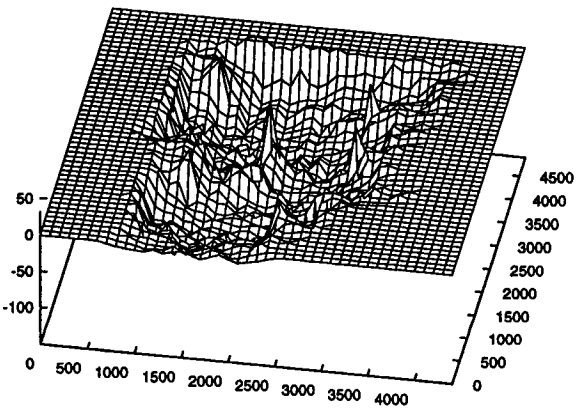

Figure 3: The mean-field score for a single edge feature, calculated after 50 timesteps of exploration in the walls environment. The grid spacing is 10cm.

Searching for plausible features

The local maxima of equation 6 correspond to plausible single features. We must now locate these maxima.

Edge features

In the case of edge features, we must find all local maxima of a function on a two dimensional space. To illustrate the difficulty of the problem, figure 3 shows a 3d plot of the mean field score against edge position, given a set of readings collected from 50 different positions within the walls environment. If we were to use a simple grid-based search to find the local maxima of this function, we would need a very high search resolution to locate every peak accurately, which would require excessive computer time.

We solve the problem by doing an exhaustive search at low (10cm) resolution, and starting a local search from each local maximum detected by the exhaustive search. For the local search we used the *simplex method* ((Press *et al.* 1993), section 10.4). We took a fractional tolerance of 0.05, and the search was abandoned if it went on for more than 50 iterations. Most searches took 20-30 iterations to find the maximum.

Wall features

The space of wall feature positions is four dimensional. However, because of the simple model we took for the effect of wall endpoint positions on sonar response, it is possible to reduce the dimension of the space that must be exhaustively searched to 2.

To reduce the search dimension, we use a special coordinate system to describe the position of a wall (figure 4). We find the positions of plausible wall features by exhaustively looping through (r_h, θ_h) space, with a resolution of $10cm$ for r_h and 30^o for θ_h. For each value of r_h and θ_h, we use a method (described below) to determine the values of l_1 and l_2 which give the highest mean-field score, and store this score. The positions of local maxima of these stored scores give approximate

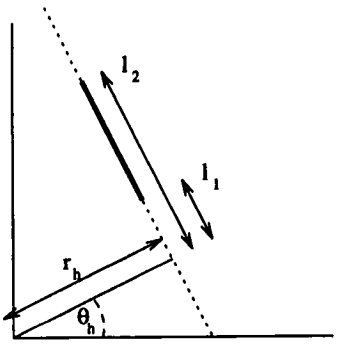

Figure 4: The coordinate system used to describe the position of wall features. The coordinates r_h and θ_h describe the infinite line of which the wall is a subsegment in Hough coordinates. l_1 and l_2 give the positions of the two endpoints, relative to the point of closest approach to the origin.

locations for plausible features and, as with edge features, a local search is started from each grid-detected local maximum.

So, given r_h and θ_h, how do we find the best endpoint positions? The effect of the wall endpoint positions l_1 and l_2 is simply to determine which readings α are included in the sum of equation 6. To find the mean-field score for any value of l_1 and l_2, we use the method illustrated in figure 5. We can find all local maxima in (l_1, l_2) space by looking for those pairs of endpoints where the left endpoint l_1 corresponds to a step up for $g(l_1)$, and the right endpoint l_2 corresponds to a step up for $f(l_2)$, subject to the constraint that $l_1 < l_2$. To find the single global maximum in this space, we simply take the largest of these local maxima.

Combining features

The methods described in the last section find local maxima of $SC_{mf}(f_0; \{r_\alpha\})$, which correspond to plausible single features in the environment.

What we want, though, is a *set* of features $\{f_i\}$ that, together, give a good score for $SC_{map}(\{f_i\}; \{r_\alpha\})$. We will find one by searching the space of all maps consisting combinations of the plausible features found by the mean-field approximation. We will use a simple iterative method. We start with an empty map. On each iteration, we loop through all plausible features, and calculate the change in map score that would be gained by adding that feature. If the best feature increases the map score, we add it and repeat the iteration; otherwise we stop.

Filtering of input data

The algorithm as described above uses *all* observations made by the robot to build a map. In theory this is will make for very accurate maps, but in practice there are two problems. The first problem is computational complexity: the amount of time taken to build a map

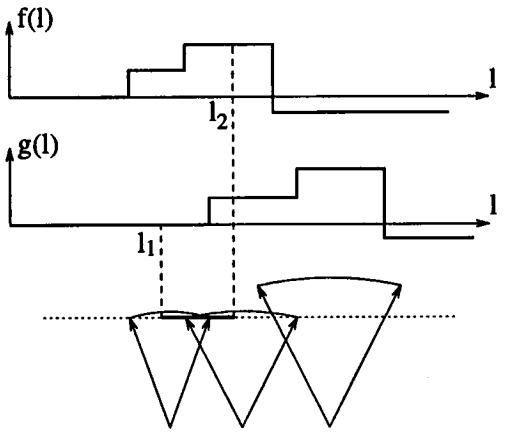

Figure 5: The method used to calculate mean field wall scores for a given choice of endpoint positions. The score $log[A_\alpha P(X_{0\alpha} \geq r_\alpha) - B_\alpha P(X_{0\alpha} > r_\alpha)]$ is computed and stored for each reading α. Two functions of l are defined: the function $f(l)$ is defined to be the sum of scores for all readings whose left beam intersection point lies to the left of l. the function $g(l)$ is defined to be the sum of scores for all readings whose right intersection point lies to the left of l. The score for a given line segment is given by $f(l_2) - g(l_1)$.

scales with the number of observations used to build it. The second problem is odometry errors. Incremental localisation will reduce these errors, but if the robot revisits a previously-explored part of the environment it is better to use the more recent readings and disregard the old ones.

To overcome these problems, we used an iterative technique to filter the readings used to make the map. A "filtered list" of readings is initialised to be empty. The observed readings are examined in reverse order, starting with the most recent. For each reading considered, if there is no reading in the filtered set taken from a viewpoint within 20cm of the current one, the current reading is added to the filtered list, otherwise it is ignored. In this way we produce a filtered list in which no two readings are taken from viewpoints within 20cm of each other, and in which more recent readings will be included over older readings.

Quantitative assessment

Performance was assessed using the map quality metric of Lee and Recce (1997). This metric compares the map derived by the robot to an ideal map that has been entered by the operator. The metric measures the fraction of a set of test journeys that the robot would complete successfully if it used its current map to plan a trajectory, but is not derived from explicit map details such as the number of features. The metric is therefore particularly sensitive to mislocated, missing or fictitious obstacles around which the robot must detour, but insensitive to obstacles which do not lie in

commonly travelled parts of space such as the corners of the room or outside the room boundaries. The metric is computed from a grid-based map of free space. Our algorithm, however, produces a list of features. We produced a grid-based map from the list of features by a similar method to that of Lee and Recce (1997) (see Harris 1999 for further details).

The new algorithm was tested on tracefiles sonar scans and movement commands collected in 3 environments by a mobile robot with a single Polaroid 6500 series rangefinder. To compare performance with existing feature-based and grid-based systems, the same data was also fed the mapping systems described by (Lee & Recce 1997) and (Lim & Cho 1992). We chose the latter system rather than one of the more commonly used grid-based systems because of the presence of specular walls in our test environment.

For each environment there were 10 files, each of which corresponding to a single exploration session of approximately 100 timesteps. The environments were: A) An empty room, with some specular and some rough walls. B) The same room with internal dividing walls and obstacles. C) The same room containing several 10cm cylindrical cans. Localisation information was determined from the tracefiles using a previously described localisation system (Lee & Recce 1997).

Results

Figure 6 shows sample maps generated by the three algorithms in environment B. The maps after one and five scans show that the new method has detected more features than the system of Lee and Recce, from the same amount of data. By forty scans, both methods have detected most of the features in the environment. However, it can be seen that features are often located more accurately by the new method, particularly in the case of wall endpoints. For example, most of the side walls are closer to their correct length, and the dividing walls do not extend into the free space in the middle of the room.

The system of Lim and Cho appears to be, if anything, faster than the new algorithm in detecting environmental reflectors. However, the maps it produces have lower quality as measured by the metric of Lee and Recce. The reason for this is probably the erroneous presence of grid segments deemed occupied in free regions.

Figure 7 shows a graph of average map quality against number of scans in the 3 environments, averaged over all 10 runs, for the new system and the system of Lee and Recce. In all cases, the new system gives highest map quality in the early stages of exploration, confirming the trend seen in the specific examples of figure 6. In environments A and B, the new algorithm produces highest asymptotic map quality, again confirming the specific examples of more accurate feature positioning in figure 6. But in environment C, the new algorithm produces a lower asymptotic map quality than the algorithm of Lee and Recce. Likely reasons for this will be discussed the next section.

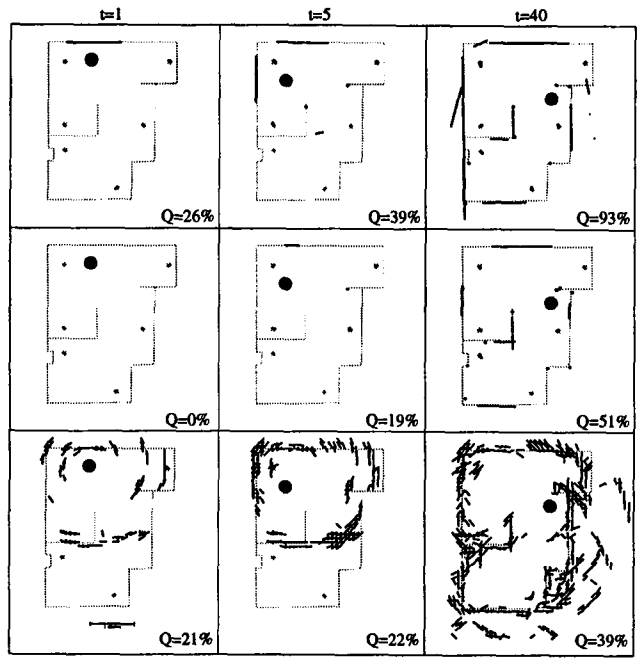

Figure 6: Some example maps built from data collected in the walls environment, after 1, 5, and 40 timesteps. The top row shows the output of the new mapping system, the second row shows the output of the system of Lee and Recce, and the third row shows the output of the system of Lim and Cho (grid segments are deemed occupied if the occupancy probability is greater than 0.5). The light lines denote the actual feature locations, and the dark lines and dots represent features detected. The large dark filled circle represents the robot. At the bottom right of each map is map quality, using the metric of Lee and Recce.

Conclusions

This paper has described a technique for mobile robot sonar mapping in which a probabilistic model of sonar behaviour is used to derive a probability function on the space of all maps, which is then searched for the map of highest probability. A mean-field approximation is used to find the positions of plausible features in the environment. A map consisting of a suitable subset of these features is then found using a iterative process.

The performance of the new technique was quantitatively compared to two previous techniques. It was found that, for all environments, the new technique produces highest map quality in the early stages of exploration, and that in two out of three of the environments tested it also produces highest asymptotic map quality.

Lower asymptotic map quality occurred in environment C, which contained several 10cm cylindrical columns. Examination of individual maps produced in this environment (not shown) showed that the cause of lower asymptotic quality was mislocalisation of these

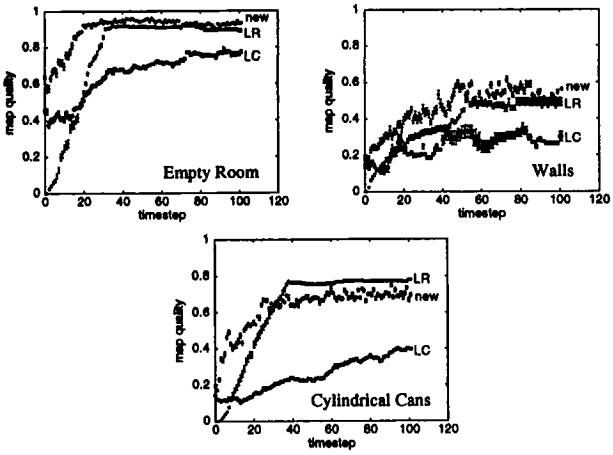

Figure 7: Average map quality against number of scans for the three methods in the three environments. The average is taken over 10 exploration runs from different starting points. Error-bars denote standard error of the mean.

columns, and that the cause of mislocalisation was most probably that the physical model used to construct the probability function did not model reflections from these columns. Future work will look at ways that the physical model may be learned from real data, allowing models for the reflection properties of a large number of objects to be constructed automatically.

Appendix - Distribution Parameters

In the case of rough walls, the distribution parameters depend on the perpendicular distance d from the sensor to the wall and the beam incidence angle θ_b through an intermediate parameter, θ_r. θ_r represents the angle of the beam portion causing the return, and is given by:

$$\theta_r = \begin{cases} \theta_b + \phi & \theta_b \leq -\phi \\ 0 & -\phi < \theta_b < \phi \\ \theta_b - \phi & \theta_b \geq \phi \end{cases} \quad (7)$$

Where $\phi = 3.4^o$. The model parameters are given by:

$$\begin{aligned} p &= 1 \\ \mu &= d/cos(\theta_r) \\ \sigma &= \Delta r_0 + \Delta\theta_r \times d \times sin(\theta_r)/cos^2(\theta_r) \end{aligned}$$

Where $\Delta r_0 = 0.5cm$ and $\Delta\theta_r = 0.02$.

Specular walls In the case of specular walls, the distribution parameters depend on perpendicular distance d and incidence angle θ_b through the modelled emitted power of the sensor, $P(\theta)$, which is given by:

$$P(\theta) = \left[\frac{2J_1(kasin(\theta))}{kasin(\theta)}\right]^2$$

where $ka = 15.5$. The distribution parameters are

$$p = \frac{1}{1 + e^{-\alpha_s - \beta_s logP(\theta_b)}}$$

$$\begin{aligned} \mu &= d + \eta_s + \zeta_s logP(\theta_b)^2 \quad (8) \\ \sigma &= \sigma_s \end{aligned}$$

where $\alpha_s = 14.38$, $\beta_s = 2.83$,$\eta_s = -4.22$, $\zeta_s = 0.10$, and $\sigma_s = 1.26$.

Sharp edges In the case of sharp edges, the distribution parameters depend on the distance d from the sensor to the edge, and incidence angle θ through a different power function $P(\theta, d)$ defined by

$$P(\theta, d) = \frac{\lambda}{d}\left[\frac{2J_1(kasin(\theta))}{kasin(\theta)}\right]^2$$

The distribution parameters are given by equations 9, but with $P(\theta_b)$ replaced by $P(\theta_b, d)$, and $\alpha_e = 21.24$, $\beta_e = 3.33$, $\eta_e = 0.023$, $\zeta_e = 0.056$, and $\sigma_e = 0.73$.

References

Antelman, G. 1997. *Elementary Bayesian Statistics.* Edward Elgar.

Elfes, A. 1987. Sonar-based real-world mapping and navigation. *IEEE J. Robotics and Automation* 3:249–265.

Harris, K., and Recce, M. 1997. Neural model of a grid-based map for robot sonar. In *proceedings of the 1997 IEEE international Symposium on Computational Intelligence in Robotics and Automation*, 34–39.

Harris, K., and Recce, M. 1998. Experimental modelling of time-of-flight sonar. *Robotics and Autonomous Systems* In press.

Harris, K. 1998. Closed-form probabilistic models of time-of-flight sonar. In *Proceedings of the 1998 European Simulation Multiconference.*

Harris, K. 1999. *Spatial function in animals and robots.* Ph.D. Dissertation, Univ. College London.

Howard, A., and Kitchen, L. 1996. Generating sonar maps in highly specular environments. In *Proceedings of the Fourth International Conference on Control, Automation, Robotics, and Vision.*

Konolige, K. 1997. Improved occupancy grids for map building. *Autonomous Robots* 4:351–367.

Lee, D., and Recce, M. 1997. Quantitative evaluation of the exploration strategies of a mobile robot. *Int. J. Robotics Research* 16:413–447.

Leonard, J. J., and Durrant-Whyte, H. F. 1992. *Directed sonar sensing for mobile robot navigation.* Cambrage, MA: Kluwer Academic Publishers.

Lim, J. H., and Cho, D. W. 1992. Physically based sensor modeling for a sonar map in a specular environment. In *Proceedings of the 1992 IEEE international conference on robotics and automation*, 1714–1719.

Moravec, H. P. 1988. Sensor fusion in certainty grids for mobile robots. *AI Magazine* 9:61–74.

Press, W.; Flannery, B.; Teukolsky, S.; and Vetterling, W. 1993. *Numerical recipes in C.* Cambridge University Press.

Thrun, S. 1998. Learning metric-topological maps for indoor mobile robot navigation. *Artificial Intelligence* 99:21–71.